



ACADEMIC
PRESS

Available online at www.sciencedirect.com

SCIENCE @ DIRECT®

Journal of Solid State Chemistry 173 (2003) 109–113

JOURNAL OF
SOLID STATE
CHEMISTRY

<http://elsevier.com/locate/jssc>

Microwave plasma growth and high spatial resolution cathodoluminescent spectrum of tetrapod ZnO nanostructures

Xian-Hua Zhang,^a Su-Yuan Xie,^{a,*} Zhi-Yuan Jiang,^a Zhao-Xiong Xie,^a Rong-Bin Huang,^a Lan-Sun Zheng,^a Jun-Yong Kang,^b and Takashi Sekiguchi^c

^aState Key Laboratory for Physical Chemistry of Solid Surfaces, Department of Chemistry, Xiamen University, Xiamen 361005, China

^bDepartment of Physics, Xiamen University, Xiamen 361005, China

^cNanomaterials Laboratory, National Institute for Materials Science, Sengen 1-2-1, Tsukuba 305-0047, Japan

Received 20 October 2002; received in revised form 21 January 2003; accepted 31 January 2003

Abstract

A novel microwave plasma assisted by tube furnace heating system is designed to grow tetrapod ZnO nanostructures. Under optimal reaction conditions, Zn powder is oxidated to form the tetrapod ZnO with straight and uniform four legs (nanorods), bearing diameters ranging from 10 to 25 nm and lengths up to 160 nm. High-resolution transmission electron microscopy analyses reveals that the tetrapod ZnO nanostructures are perfect crystalloid. High spatial resolution cathodoluminescent spectrum for individual tetrapod ZnO nanostructure shows only a strong ultraviolet emission at 385 nm.

© 2003 Elsevier Science (USA). All rights reserved.

Keywords: Cathodoluminescence; Microwave; Nanostructures; Plasma; ZnO

1. Introduction

Nanoscale ZnO is intensively studied for its outstanding electronic and optical properties. A wide variety of approaches have been developed for the synthesis of various ZnO nanomaterials, such as nanoparticles [1], nanorods [2,3], nanobelts [4] and nanowires [5,6]. Potential applications of ZnO nanostructures have been investigated in nanotechnology fields, such as nanolaser [7] and optical switch [8]. Recently, assembly of ZnO nanomaterials attracts increasing attentions partly due to the improving properties of assembled nanostructures. For instance, room-temperature UV lasing properties have been demonstrated in ZnO nanowire array material [7], which is self-assembled from nanowires. Synthesis and assembly of novel ZnO nanostructures are still of importance for the nanotechnology and remain to be a challenge for chemists and physicists.

Tetrapod-like ZnO structures attract continuous attentions for both their fascinating structure and potential applications. Large tetrapod-like ZnO crystals

have been synthesized for many years [9]. Some efforts to the synthesis of tetrapod ZnO in nanoscale have been reported recently [10,11], and application researches on such a kind of nanostructure are in progress, e.g. ZnO–glass varistor [11]. These promising findings stimulate the interest of scientists to synthesize tetrapod ZnO nanostructures via different techniques. Here an effective microwave plasma system is designed to grow symmetric tetrapod ZnO nanostructure, in which four nanorods (legs) with diameters ranging 10–25 nm and lengths up to 160 nm are self-assembled at one common juncture.

2. Experimental section

The tetrapod ZnO was synthesized and self-assembled from Zn oxidation in the microwave plasma assisted by a tube furnace heating system (Fig. 1). Two grams of zinc powder was put into a quartz boat, and the boat was placed into the center of a horizontal quartz tube with 3 cm diameter and 30 cm length, which act as the reactor chamber in the experiments. Ar (30 sccm) and O₂ (20 sccm) were used as carrier gas and reactant gas,

*Corresponding author. Fax: +86-592-218-3047.

E-mail address: syxie@jingxian.xmu.edu.cn (S.-Y. Xie).

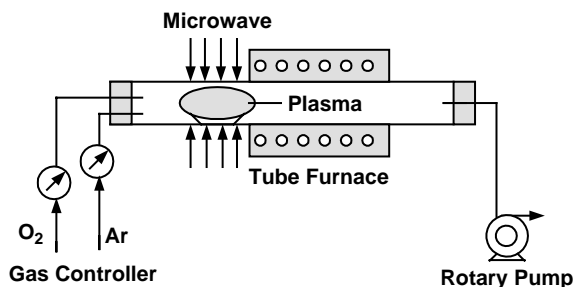


Fig. 1. Schematic illustration of microwave plasma system.

respectively. The reactor chamber pressure was maintained at about 4 Torr by a rotary pump. A 400 W 2.45 kHz microwave source was introduced along a square rectangle wave-conduct pipe to couple the microwave to the quartz tube center for generating stable plasma. The temperature of microwave plasma was estimated above 1000°C. To obtain appropriate temperature zone and gradient, a tube furnace with length of 20 cm was mounted on the downstream end of the quartz tube as an assistant heating source. The center temperature of the assistant tube furnace was 600°C, and the temperature inside the quartz tube was estimated about 450°C. After reaction for 20 min, the microwave system was turned off and the furnace was gradually cooled to room temperature. About 2.4 g as-prepared white products on the inner-wall of the quartz tube were collected for characterization, in which the yield of tetrapod ZnO nanostructures was about 75%.

X-ray powder diffraction (XRD) was carried out on a Rigaku DMAX/RC X-ray diffractometer using $\text{CuK}\alpha$ radiation ($\lambda = 0.154178$ nm). Transmission electron microscopy (TEM) micrographs were taken using a JEM-100CXII TME. High-resolution transmission electron microscopy (HRTEM) images were obtained on a JEOL-2010 TEM. Cathodoluminescent (CL) spectrum was performed on a high spatial resolution CL system. A scanning electron microscope (SEM) equipped with a thermal field emission (TFE) gun to supply the electron beam current of 1 nA operating at 1 kV, and the TFE-SEM (Hitachi 4200) was customized for low energy CL (LE-CL) system. The high spatial resolution CL system was operated at low electron beam energies using TFE-SEM [12].

3. Results and discussion

TEM image of the products (Fig. 2) shows each nanostructure is assembled by four nanorods, with diameters ranging from 10 to 25 nm and lengths up to 160 nm, which are linked to each other at one end to form tetrapod-like structure. From the tetrapod nanostructure as indicated at arrowhead point, in which

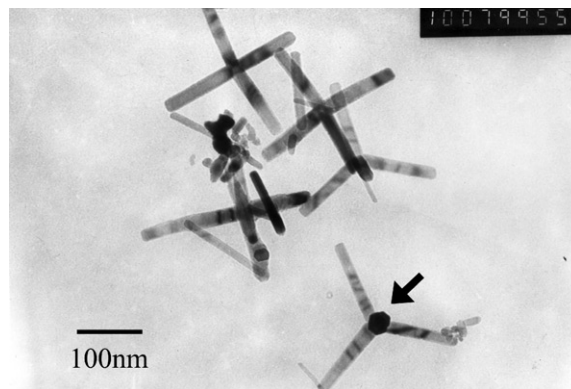


Fig. 2. Typical TEM image of the tetrapod ZnO nanostructures.

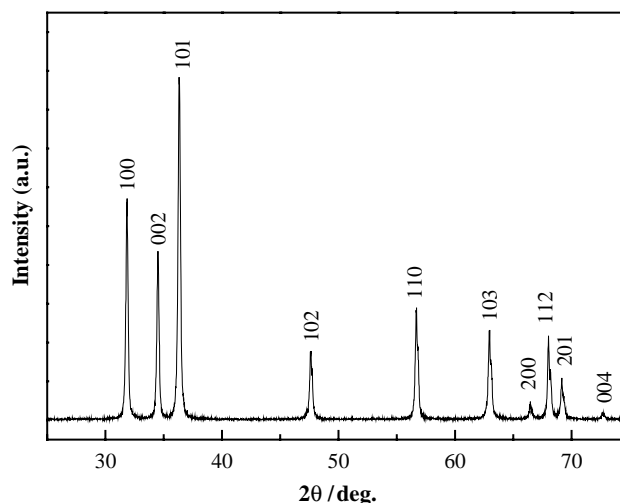


Fig. 3. Typical XRD pattern of the tetrapod ZnO nanostructures.

one leg perpendicularly sticks out the paper plane, the cross-section of the nanorod exhibits hexagonal shaped.

The crystallinity and purity (composition and phase) of the as-prepared tetrapod junction structures was determined by XRD. Fig. 3 shows the XRD pattern where all diffraction peaks are well indexed to the hexagonal ZnO phase (JCPDS No. 36-1451).

Further structural information of the junction in the tetrapod ZnO nanostructure was revealed by HRTEM images. Fig. 4a shows a typical HRTEM image taken in an appropriate orientation, in which the fourth leg is hidden from view so that a better lattice image is observed. One can observe that the lattices near the junction exhibit continuous without cracks, confirming the junction with perfectly crystalline structure. As shown in Fig. 4b, corresponding to the left nanorod of the tetrapod ZnO appeared in Fig. 4c, the crystal lattice in the body of the nanorod is perfect. The fringes are perpendicular to the long direction of the nanorod, and the singular fringe spacing is about 0.51 nm, which is nearly consistent with the *c*-axis parameter

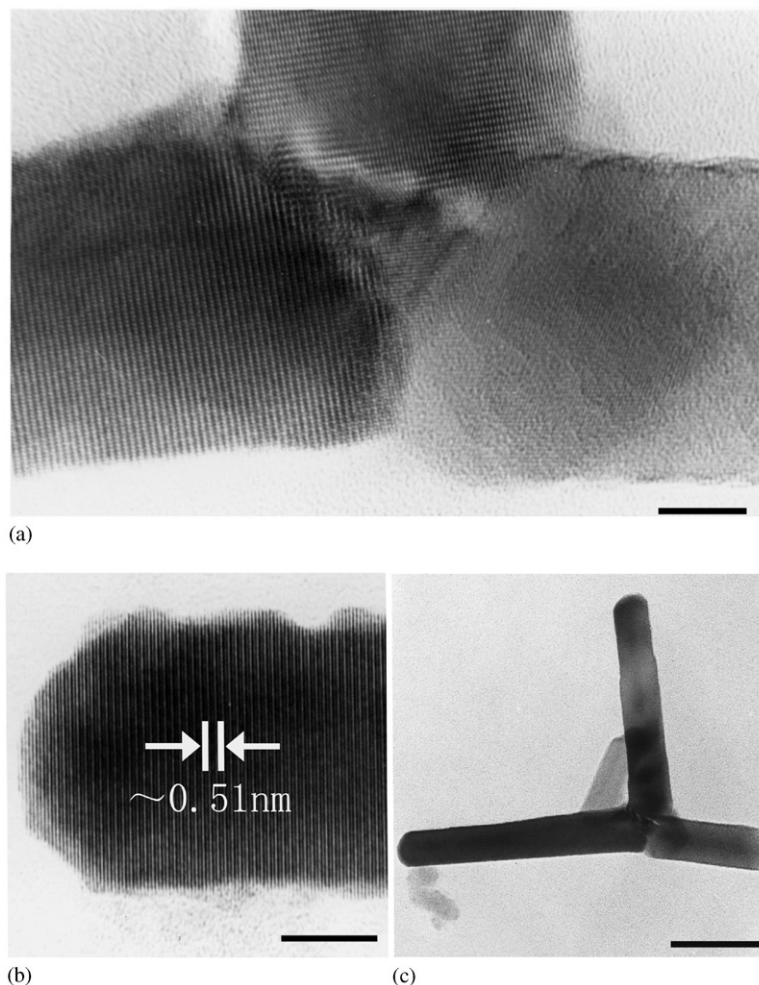


Fig. 4. (a) HRTEM image of the junction in a selected tetrapod ZnO nanostructure (scalebar = 6 nm); (b) HRTEM image of one nanorod (leg) in the selected tetrapod ZnO nanostructure (scalebar = 6 nm); (c) TEM image of the selected ZnO tetrapod nanostructure with the junction shown in Fig. 4a and the nanorod shown in Fig. 4b (scalebar = 50 nm).

($c = 0.521$ nm) in hexagonal ZnO structure, implying the nanorod grow along [001] direction.

To obtain the exactly optical properties of individual tetrapod ZnO nanostructure, a high spatial resolution cathodoluminescence system operating under low electron beam energies using thermal field-emission gun is employed. Since a low energy electron beam strongly reduces the electron range, the spatial resolution of the CL system is ca. 100 nm in the actual operation at 3 kV. Thus, it is appropriate for the optical characterization of as-prepared tetrapod ZnO nanostructures. Fig. 5 shows the high spatial resolution CL spectrum of individual tetrapod ZnO nanostructure, which exhibited strong ultraviolet (UV) emission centered at 385 nm. The UV emission is attributed to the near band edge emission of the wide band-gap ZnO. Compared with the optical properties of the similar tetrapod ZnO structures synthesized by the other techniques [10], the defect emission (around 550 nm) is invisible. The result supports that the as-synthesized tetrapod ZnO nanostructures bear perfect crystallinity.

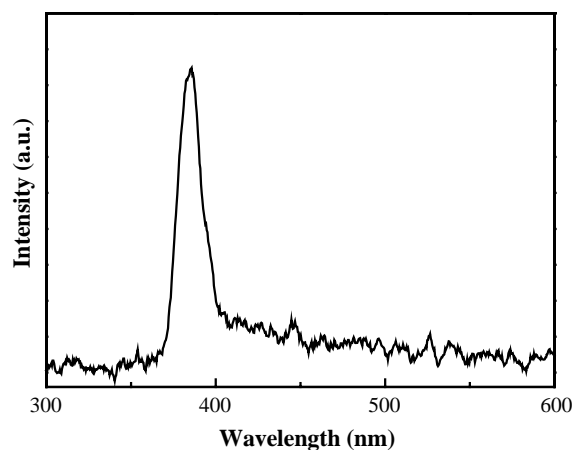


Fig. 5. High spatial resolution CL spectrum of individual tetrapod ZnO nanostructure.

The growth of the uniform tetrapod ZnO nanostructures depends on both reaction temperature (zone and gradient) and gas flows. As shown in Fig. 6a, irregular

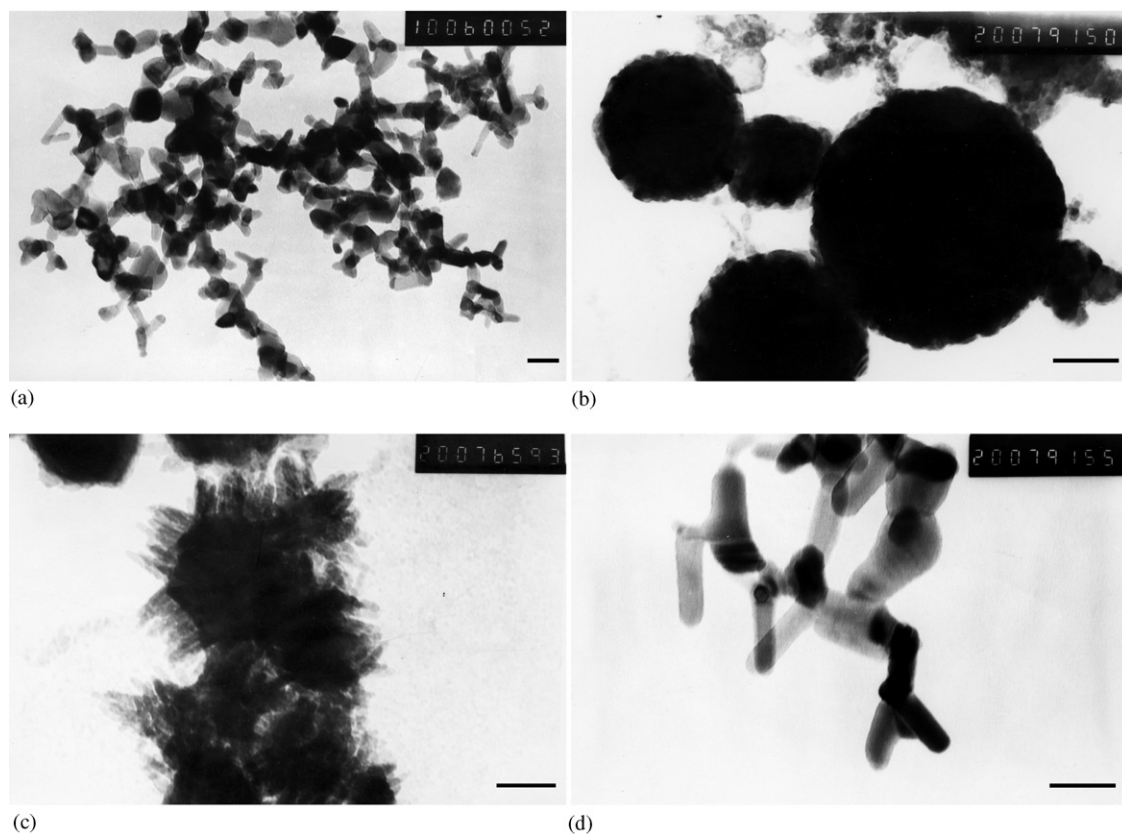


Fig. 6. TEM images of ZnO nanostructures growth under different reaction conditions: (a) 20 sccm O₂, 30 sccm Ar, no assistant heating by tube furnace. (b) 1 sccm O₂, 100 sccm Ar, no assistant heating by tube furnace. (c) 1 sccm O₂, 80 sccm Ar, no assistant heating by tube furnace. (d) 20 sccm O₂, 60 sccm Ar, assistant heating by tube furnace. (The center temperature of the tube furnace was 600°C, and the temperature inside quartz tube was estimated about 450°C.) (scalebar = 50 nm).

nanoparticles and pre-matured multi-legs nanostructures were dominant when Zn oxidation in the microwave plasma system without assistant tube furnace employed. High yield of the uniform tetrapod ZnO were obtained while a tube furnace with temperatures of 600°C was mounted around the quartz tube behind the microwave plasma zone. In addition to temperature parameter, the carrier gas flow and oxygen gas concentration also affect the morphologies of the products in the microwave plasma process. To examine the influence of the flows of Ar and O₂ on the morphologies of the products (Figs. 6b and d), the flows are controlled using gas flowmeters. Morphology analysis reveals that smaller gas flow, accompanying appropriate temperature gradient and heating zone, is benefit to the formation of tetrapod ZnO nanostructures. Finally, the flow values of Ar and O₂ are optimized to be 30 and 20 sccm, respectively.

Growth of large tetrapod ZnO crystal has been investigated in previous paper [13]. The octahedral nuclei were initially formed, and continuously grown up with increasing internal stress. The crystals were expelled out of the grain boundary when they became

unable to resist the internal stress. The emerged octahedral crystals began to develop their legs on their alternative faces to form large and uniform tetrapod-like crystals in the vapor of zinc and oxygen. In the present case, no metal catalyst was used, so the as-prepared tetrapod ZnO nanostructures are believed to undergo the vapor nucleation and the succeeding legs, which is similar to the formation mechanism of large tetrapod ZnO crystals. The HRTEM results reveal that the nanorod grow preferably along to the certain direction, i.e. [001] direction.

Although no catalyst is employed in the present experiment, tetrapod ZnO nanostructures obtained with high yield (>75%) in the microwave plasma system, this may be related with so-called “microwave effect” [14]. The advantages associated with microwave processing include: rapid and stable heating; decreased sintering temperatures; and some properties unobserved in conventional processes [14]. In the present experiment, Zn powder can be evaporated rapidly (within about 10 s). The instantaneous evaporation could reduce dramatically the oxidation of Zn reactant on the surface during the process leading to inhomogeneous zinc evaporation.

Acknowledgments

This work was supported by Chinese National Natural Science Foundation (Grant 20001005, 20273052, 20023001 and 20021002), the Major State Basic Research Development Program (2002CCA01600) and the Natural Science Foundation of Fujian Province (No. E0010001). We thank Ms. Zi-Mian Ni, Ms. Ru Xue, and Dr. He-Sheng Zhai from Analytic Center of Xiamen University for TEM analyses. The authors also thank Prof. Shu-Yuan Zhang from University of Science and Technology of China for HRTEM measurements.

References

- [1] L.F. Dong, L.Z. Cui, Z.K. Zhang, *Nanostruct. Mater.* 8 (1997) 815.
- [2] J.J. Wu, S.C. Liu, *Adv. Mater.* 14 (2002) 215.
- [3] C. Pacholski, A. Kornowski, H. Weller, *Angew. Chem. Int. Ed.* 41 (2002) 1188.
- [4] Z.W. Pan, Z.R. Dai, Z.L. Wang, *Science* 291 (2001) 1947.
- [5] J. Zhang, L.D. Sun, H.Y. Pan, C.S. Liao, C.H. Yan, *New J. Chem.* 26 (2002) 33.
- [6] Y.C. Kong, D.P. Yu, B. Zhang, W. Fang, S.Q. Feng, *Appl. Phys. Lett.* 78 (2001) 407.
- [7] M.H. Huang, S. Mao, H. Feick, H.Q. Yan, Y.Y. Wu, H. Kind, E. Weber, R. Russo, P.D. Yang, *Science* 292 (2001) 1897.
- [8] H. Kind, H.Q. Yan, B. Messer, M. Law, P.D. Yang, *Adv. Mater.* 14 (2002) 158.
- [9] M. Kitano, T. Hamebe, S. Maeda, T. Okabe, *J. Cryst. Growth* 102 (1990) 965.
- [10] Y. Dai, Y. Zhang, Q.K. Li, C.W. Nan, *Chem. Phys. Lett.* 358 (2002) 83.
- [11] J. Wu, C.S. Xie, Z.K. Bai, B.L. Zhu, K.J. Huang, R. Wu, *Mater. Sci. Eng. B-Solid* 95 (2002) 157.
- [12] T. Sekiguchi, K. Sumino, *Rev. Sci. Instrum.* 66 (1995) 4277.
- [13] M. Kitano, T. Hamebe, S. Maeda, T. Okabe, *J. Cryst. Growth* 108 (1991) 277.
- [14] D.E. Clark, D.C. Folz, J.K. West, *Mater. Sci. Eng. A-Struct.* 287 (2000) 153.